Seasonal Variation in the MINOS Detectors

J.K. de Jong [*†],E.W. Grashorn[‡§]for the MINOS collaboration

[*]*Illinois Institute of Technology,Chicago Illinois 60616 USA*
[†]*now at University of Oxford, Oxford OX1 3RH United Kingdom*
[‡]*School of Physics and Astronomy, University of Minnesota,Minneapolis,MN 55455*
[§]*now at Center for Cosmology and AstroParticle Physics, Ohio State University, Columbus, OH 43210*

Abstract. **The MINOS Near and Far Detectors have both observed seasonal variations in the underground muon rate (R_μ). This variation is correlated to the change in the temperature of the upper atmosphere. With five years of Far Detector data and two-and-a-half years of Near Detector data this correlation, α_T=$(T/R_\mu)(\partial R_\mu/\partial T)$, is measured to be 0.874$\pm$0.009(stat.)$\pm$0.010(syst.) and 0.43$\pm$0.03(stat.) respectively.**

Keywords**: MINOS, Seasonal Variations**

I. Introduction

When high energy cosmic ray primaries interact with nuclei in the upper atmosphere the subsequent shower produces kaons (K) and pions (π). These secondary mesons can either interact and produce low energy hadronic cascades, or decay to muons. It is these high energy muons which are observed by underground detectors. The probability that a secondary meson will decay is dependent, in part, on the meson energy E_M as well as the effective atmospheric density ρ through which it travels. While the surface temperature changes dramatically during any given day, the temperature of the stratosphere, the region of the atmosphere where the bulk of the primary interactions occur, changes tend to occur gradually over the course of the seasons. Increases in the temperature of the stratosphere decrease the density which reduces the probability that a secondary meson will interact before it has the opportunity to decay and thus the observed muon rate increases[1][2][3]. Furthermore, the seasonal effect increases as higher energy muons are sampled as they come from more energetic mesons which have increased lifetimes.

MINOS is a two detector long baseline neutrino beam oscillation experiment[4]. The ν_μ source and Near Detector are located at Fermi National Accelerator Laboratory in Batavia, IL. The Far Detector is situated in the Soudan Underground Mine State Park in Soudan, MN. Each detector is a scintillator and steel tracking calorimeter with tracking, energy and topology measurement capabilities. The 0.98 kton Near Detector is used to characterize the spectrum of the neutrino beam and is located in a cavern 94 m underground at the end of the NuMI beam facility (approximately 1 km from the primary proton target). The 5.4 kton Far Detector is located 734 km further downstream and is 0.72 km below the surface. The Near Detector has a flat overburden of 224 meters of water equivalent(mwe); to reach the Near Detector muons require a minimum energy of 0.05 TeV. The Far Detector overburden at its minimum is 2100 mwe and has a surface energy threshold of 0.73 TeV. Prior to any analytical selections the cosmic ray muon trigger rates are 0.5364$\pm$0.0001 Hz at the Far Detector and 27.29$\pm$0.01 Hz at the Near Detector. The data is observed to be consistent with the rates expected from Poisson distributions for random processes.

The atmospheric temperature to muon intensity relationship can be expressed [1]:

$$\frac{\Delta I_\mu}{I_\mu^0} = \int_0^\infty dX \alpha(X) \frac{\Delta T(X)}{T}, \qquad (1)$$

where ΔI_μ is the deviation from the overall average muon intensity, I_μ^0 is the muon intensity evaluated at a given temperature T, and $\alpha(X)$ is the coefficient relating changes in temperature to changes in intensity as a function of slant depth X, the path length through the atmosphere. Figure 1 shows how the temperature above the Near Detector varies continuously as a function of slant depth. Notice that some levels have a greater variation in temperature than do others. The temperature as a function of slant depth for both the Near and Far Detectors has been determined using the European Centre for Medium-Range Weather Forecasts(ECMWF) global atmospheric model[5]. The model provides atmospheric temperatures at 21 different pressure levels between 1 and 1000 hPa at four different times (0000 h,0600 h,1200 h and 1800 h) throughout the day. Above 1 hPa the density of the atmosphere is insufficient to produce a statistically significant number of the mesons that decay to muons.

It is impossible for the MINOS detectors to determine where in the atmosphere the detected muon was produced. To simplify calculations the atmosphere is approximated by an isothermal body with a single effective temperature T_{eff}. This temperature is determined from a weighted average of the pressure levels where the weights reflect the probability of a meson being produced at that pressure level and decaying to produce a muon. The first quantity is determined by the cosmic

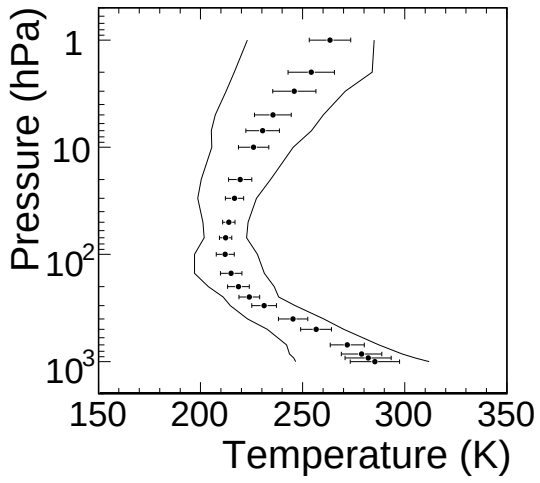

Fig. 1. The data points represent the average temperature above the Near Detector at that pressure level over a 3 year period commencing January 2006; the error bars are the one sigma standard deviation. The lines on either side of the plot represent the extrema of the temperature reached during the time interval.

ray primary, the second by the energy and type of meson produced.

II. Seasonal Variations

At the muon energies observed at the MINOS Far Detector the Kaon contribution to the differential muon spectrum[6] must be considered. In this case the total change in intensity for high energy muons is:

$$\Delta I_\mu \equiv \int_0^\infty dX \alpha^\pi(X) \frac{\Delta T(X)}{T_{\rm eff}} e^{X/\Lambda_\pi} + \int_0^\infty dX \alpha^K(X) \frac{\Delta T(X)}{T_{\rm eff}} e^{X/\Lambda_K}. \quad (2)$$

The temperature coefficient $\alpha^{\pi,K}(X) = W^{\pi,K}(X) E_{th}^{-\gamma}$ and $W^{\pi,K}(X)$ is written [7]:

$$W^{\pi,K}(X) \simeq \frac{(1 - X/\Lambda'_{\pi,K})^2 e^{-X/\Lambda_{\pi,K}} A^1_{\pi,K}}{\gamma + (\gamma+1) B^1_{\pi,K} K(X) \left(E_{th} \cos\theta/\epsilon_{\pi,K}\right)^2}, \quad (3)$$

where

$$K(X) \equiv \frac{(1 - X/\Lambda'_{\pi,K})^2}{(1 - e^{-X/\Lambda'_{\pi,K}})\Lambda'_{\pi,K}/X} \quad (4)$$

and $T_{\rm eff}$ is the effective temperature, the temperature of an isothermal atmosphere, $1/\Lambda'_{\pi,K} \equiv 1/\Lambda_N - 1/\Lambda_{\pi,K}$, $\Lambda_N = 120\,{\rm g/cm^2}$, $\Lambda_\pi = 160\,{\rm g/cm^2}$ and $\Lambda_K = 180\,{\rm g/cm^2}$ [6] and meson critical energies $\epsilon_\pi = 0.114\,{\rm TeV}, \epsilon_K = 0.851\,{\rm TeV}$.

Letting $T_{\rm eff}$ be defined such that when $T(X) = T_{\rm eff}$, $\Delta I_\mu = 0$, an expression for $T_{\rm eff}$ can be found:

$$T_{\rm eff} = \frac{\int_0^\infty dX T(X) \alpha^\pi(X) + \int_0^\infty dX T(X) \alpha^K(X)}{\int_0^\infty dX \alpha^\pi(X) + \int_0^\infty dX \alpha^K(X)} \quad (5)$$

Since the temperature is measured at discrete levels, the integral reduces to a sum over the atmospheric levels X_n:

$$T_{\rm eff} \simeq \frac{\sum_{n=0}^N \Delta X_n T(X_n) \left(W_n^\pi + W_n^K\right)}{\sum_{n=0}^N \Delta X_n \left(W_n^\pi + W_n^K\right)} \quad (6)$$

.

The observed muon rate($R_\mu = N_\mu/\Delta t$) at the detector is correlated with the incident muon flux:

$$R_\mu = \int I_\mu(\cos\theta,\phi) \epsilon(\cos\theta,\phi) A_{\rm tot}(\cos\theta,\phi) {\rm d}\cos\theta {\rm d}\phi, \quad (7)$$

where $A_{\rm tot}$ is the total effective area of the detector, ϵ is the efficiency, and the expression is integrated over the angles $\cos\theta, \phi$. Since the configuration and acceptance do not vary the change in muon rate is directly related to the change in intensity and can be written: $\frac{\Delta I_\mu}{I_\mu} = \frac{\Delta R_\mu}{R_\mu}$. Finally we obtained a simplified relationship between atmospheric temperature fluctuations and intensity variations which can be written:

$$\int_0^\infty dX \alpha(X) \frac{\Delta T(X)}{T(X)} = \alpha_T \frac{\Delta T_{\rm eff}}{\langle T_{\rm eff}\rangle} = \frac{\Delta R_\mu}{\langle R_\mu\rangle}. \quad (8)$$

III. Data Analysis

This analysis uses five years of Far Detector data collected between August 1, 2003 and August 1, 2008 and 510 days of Near Detector data collected between January 1, 2006 and September 6, 2008. During these time intervals the mean observed muon rate was $< R_\mu >$=0.5364±0.0001 Hz and 27.29±0.01 Hz at the Far and Near Detectors respectively.

Data quality cuts are included to ensure a clean sample of muons; for the Far Detector analysis these selections are detailed in [15]. Data quality cuts ensure that the detector is in a good state during which the data is being taken. These criteria reduce the Far Detector data sample from 68.66 million muons to 67.32 million, and the muon rate to $< R_\mu >$=0.4692±0.0001 Hz. Figure 2(top) plots the observed daily deviation, $\frac{\Delta R_\mu}{<R_\mu>} = \frac{(R_{day} - <R_\mu>)}{<R_\mu>}$, in the Far Detector muon rate from the mean value as a function of calendar date. The muon rate variation with season is clearly observed with maxima in August and minima in February. The muon rate for any given day R_{day} is the number of muons counted divided by the livetime in seconds for that day. with the error being the square root of the number of events divided by the livetime.

For the Near Detector analysis both data quality and track quality cuts have been applied. After these selections the average muon rate for this time period was $< R_\mu >$=0.8286±0.0002 Hz. A more detailed discussion of the Near Detector data and track quality cuts can be found in [16].

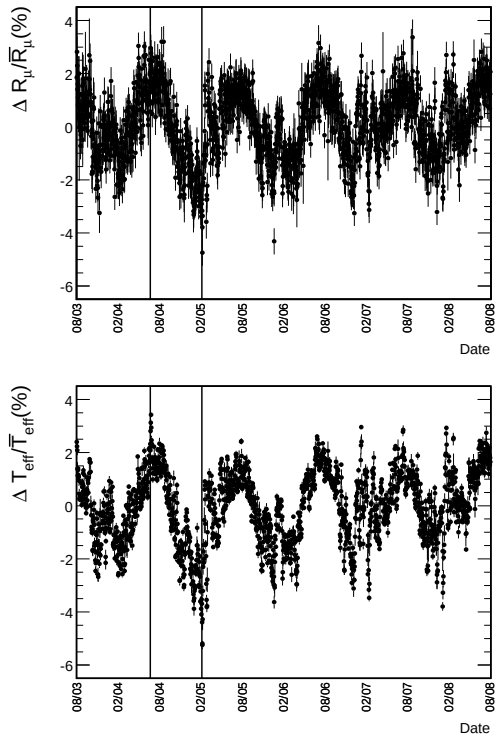

Fig. 2. The daily deviation from the mean rate (top) and from mean effective temperature$< T_{eff} >$(bottom) observed in the Far Detector from 8/03-8/08. The periodic fluctuations have the expected maxima in August, minima in February. The vertical bars indicate the period of time when the detector ran in nominal reverse field mode.

The effective temperatures for both the Near and Far Detectors are determined using equation 5 and the relevant ECMWF data. $T_{\rm eff}$ was calculated four times each day using this method and then averaged. The daily statistical error on $T_{\rm eff}$ was estimated by calculating $\sigma^2 = \left\langle T_{\rm eff}^2 \right\rangle - \left\langle T_{\rm eff} \right\rangle^2$. For the Near Detector an extra error of ± 0.5 K was added in quadrature with the statistical error to account for discrepancies with other atmospheric Temperature measurements[18]. Over the data samples analyzed the average effective temperature above the Far Detector is calculated to be $< T_{eff} >$=222.1 K while at the Near Detector the temperature is slightly lower at 220.2 K. Figure 2(bottom) plots the observed daily deviation, $\frac{\Delta T_{eff}}{<T_{eff}>} = \frac{(T_{eff,day} - <T_{eff}>)}{<T_{eff}>}$, of the Far Detector effective temperature as a function of the calendar date. One can see that there is a strong correlation between the effective temperature and the observed daily rate on both the seasonal and short term scales[19].

The correlation coefficient, α_T, between the change in effective temperature and the change in daily muon rate can be determined with a linear fit of $\frac{\Delta R_\mu}{<R_\mu>}$ to $\frac{\Delta T_{eff}}{<T_{eff}>}$. To find the value for α_T, a linear regression was performed using ROOT's MINUIT [17] fitting package. This package performs a linear regression accounting for error bars on both the x and y axis using a numerical minimization method. Fitting the Far Detector data in figure 3 returns a slope of $\alpha_T = 0.874 \pm 0.009$. The systematic error on the Far Detector measurement was determined to be 0.010 by evaluating the effect on the slope of 1σ changes on the parameters in the determination of T_{eff}. The same fit, without a systematic error study, was done to the Near Detector data,figure 4, giving an $\alpha_T = 0.43 \pm 0.03$.

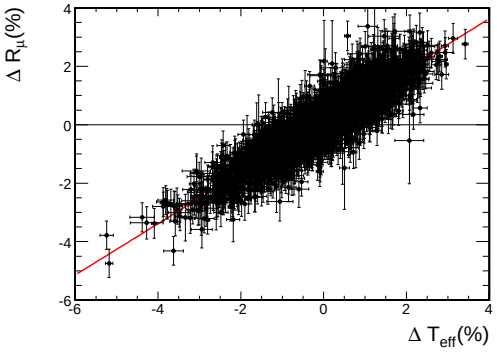

Fig. 3. A plot of $\Delta R_\mu / \langle R_\mu \rangle$ vs. $\Delta T_{\rm eff} / \langle T_{\rm eff} \rangle$ for single muons observed at the Far Detector. The fit has a $\chi^2/ndf = 1905/1797$, and the slope is $\alpha_T = 0.874 \pm 0.009$.

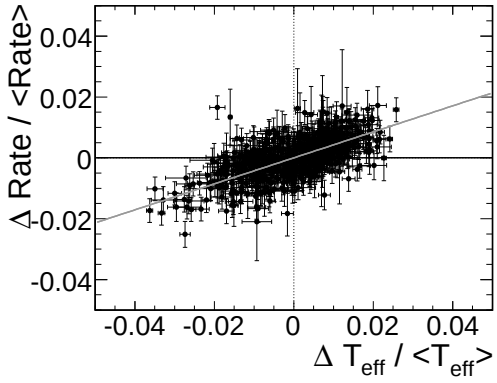

Fig. 4. This graph plots, for the Near Detector, the fractional deviation of the daily muon rate from the average (ΔR/R) versus the fractional deviation of the effective temperature from the average temperature($\Delta T/T$). The slope is α_T=0.43±0.03(stat.).

IV. Expectation

The theoretical value of α_T can be written in terms of the differential muon intensity I_μ as[1]:

$$\alpha_T = -\frac{E_{th}}{I_\mu^0}\frac{\partial I_\mu}{\partial E_{th}} - \gamma, \qquad (9)$$

Performing the differentiation[6]:

$$\alpha_T = \frac{1}{D_\pi}\frac{1/\epsilon_K + A_K^1 (D_\pi/D_K)^2/\epsilon_\pi}{1/\epsilon_K + A_K^1 (D_\pi/D_K)/\epsilon_\pi} \qquad (10)$$

where

$$D_{\pi(K)} = \frac{\gamma}{\gamma+1}\frac{\epsilon_{\pi(K)}}{1.1E_{th}\cos\theta} + 1, \qquad (11)$$

To compare the experimental α_T to the theoretical expectation, a simple *Monte Carlo* calculation was performed to find the expected average value given by Eq. 10. A muon energy and $\cos\theta$ were chosen out of the differential muon intensity [6], A random azimuthal angle, ϕ, was chosen and combined with $\cos\theta$ and the Soudan rock overburden map [15] to find the slant depth D (kmwe). The threshold surface energy required for a muon to survive this column depth is found from the expression for threshold energy [15]. If the chosen E_μ was greater than E_{th}, it was used in the calculation of the theoretical $\langle\alpha_T\rangle$. This was repeated for 10,000 successful E_μ to find $\langle\alpha_T\rangle = 0.871 \pm 0.025$ for the MINOS Far Detector, which is in agreement with the observed value.

To compare the MINOS result with other underground experiments, this process was repeated for standard rock, flat overburden, and $D = h/\cos\theta$, where h is the detector depth in mwe. 10,000 successful muons were used to find α_T at depths from 0 to 4,000 mwe. The result of this calculation, along with data from other experiments, can be seen in Fig. 5 as the solid line. This curve includes the "negative temperature effect" (muon decay correction) term, $\delta' = (1/E\cos\theta)(m_\mu c^2 H/c\tau_\mu)(\gamma/\gamma+1)\ln(1030/\lambda_p\cos\theta)$ [1], which goes to zero for $E_\mu > 50\,\mathrm{GeV}$. The theoretical prediction of α_T of the pion-

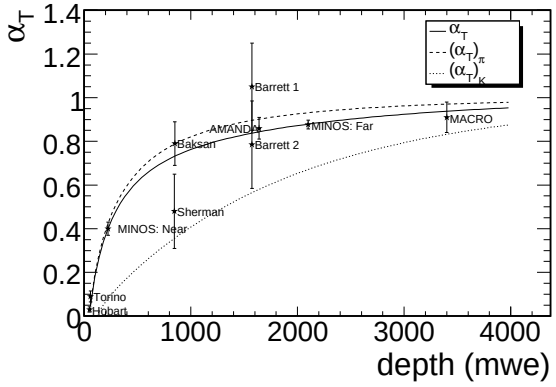

Fig. 5. The theoretical prediction for α_T as a function of detector depth. The solid (top) curve is the prediction using the pion-only model (of MACRO) and the dotted (bottom) curve is the prediction using a kaon-only model. The solid (middle) curve is the new prediction including both K and π. The data from other experiments are shown for comparison only, and are from Barrett 1, 2 [1], AMANDA [3], MACRO [8], Torino [9], Poatina [10], Utah [11] , Sherman [12], Hobart [13] and Baksan [14].

only and kaon-only model both approach 1 at high slant depths(high meson energy). At similar low energies Kaons are less susceptible to the seasonal effect and as such have a systematically lower α_T. The result is a large gap between the pion-only and the kaon-only predictions. The experimentally derived value is expected to be somewhere between these two values depending on the πK ratio. Both the observed Near and Far Detectors α_T agree with the seasonal variation model which incorporates both pions and kaons.

V. Conclusion

The MINOS Near and Far Detectors have now both observed seasonal variations in the underground muon rate, R_μ. The correlation coefficients between the observed rate and the effective temperature have been measured to be to be α_T =0.874±0.009(stat.)±0.010(syst.) and α_T =0.43±0.03(stat.) at the Far(2100 mwe) and Near Detectors(220 mwe) respectively. These observations are consistent with the theoretical expectation which includes contributions from both pions and kons.

VI. Acknowledgements

This work was supported by the US DOE, the UK STFC, the US NSF, the State and University of Minnesota, the University of Athens, Greece and Brazil's FAPESP and CNPq. We are grateful to the Minnesota Department of Natural Resources, the crew of Soudan Underground Laboratory, and the staff of Fermilab for their contributions to this effort.

References

[1] P. Barrett *et al.*, Reviews of Modern Physics **24**133(1952)
[2] M. Ambrosio *et al.*(MACRO), Astropart. Phys. **7** 109(1997)
[3] A. Bouchta *et al.*(AMANDA)(1999), prepared for the 26th International Cosmic Ray Conference (ICRC 99) Salt Lake City,UT, 17-25 Aug
[4] D. G. Michael *et al.*(MINOS)., Nucl. Instr. & Meth. A **596**,190(2008)
[5] European Centre for Medium-Range Weather Forecasts ECMWF Operational Analysis data,[Internet] British Atmospheric Data Centre,**2006-2007**(Available from http://badc.nerc.ac.uk/data/ecmwf-op/).
[6] T.K. Gaisser(1990), cambridge UK:Univ Pr. (1990) 279 p.
[7] E. W. Grashorn(2008) PhD Dissertation, University of Minnesota FEMILAB-THESIS-2008-06
[8] M. Ambrosio *et al.*(MACRO) Phys. Rev. **D67**, 042002(2003),astro-ph/0211119.
[9] G.C Castagnoli and M.Dodero,Il Nuovo Cim **B51**(1967).
[10] J. Humble *et al* Proc. 16th ICRC (Kyoto) **4**(1979)
[11] D. Cuter *et al* Proc. 17th ICRC (Paris) **4**(1981)
[12] N. Sherman, Phys. Rev **93**(1954)
[13] A. Fenton,R. Jacklyn and R.Taylor, Il Nuovo Cimento **B22** (1961)
[14] Y. Andreyev *et al*. Proc. 20th ICRC(Moscow) **9** (1990)
[15] P. Adamson *et al.*(MINOS) Phys. Rev **D76**,052003(2007), arXiv:0705.3815 [hep-ex].
[16] J.K. de Jong *et al.*(MINOS) These proceedings.
[17] F. James and M. Roos,Comput. Phys. Commun. **10**,343(1975)
[18] I. Durre, R.S. Vose and D.B. Wuertz,*Overview of the integrated global radiosonde archive*, Journal of Climate, **19**:53-68,2006
[19] S. Osprey *et al.*(with MINOS) Geophysical Research Letters **36**,L05809, doi:10.1029/2008GL036359, 2009.